# Electronic and magnetic properties of $CoFeV_{0.5}Mn_{0.5}Si$: experiment and theory

Parashu Kharel,[1,#] Gavin Baker,[1] Matthew Flesche,[1] Adam Ramker,[2]

Shah Valloppilly[3], Paul M. Shand,[2] and Pavel V. Lukashev[2,*]

[1]*Department of Physics, South Dakota State University, Brookings, SD 57007, USA*

[2]*Department of Physics, University of Northern Iowa, Cedar Falls, IA 50614, USA*

[3] *Nebraska Center for Materials and Nanoscience, University of Nebraska, Lincoln, NE 68588, USA*

# parashu.kharel@sdstate.edu

* pavel.lukashev@uni.edu

## Abstract

Half-metallic Heusler alloys have attracted significant attention due to their potential application in spin-transport-based devices. We have synthesized one such alloy, $CoFeV_{0.5}Mn_{0.5}Si$, using arc melting and high-vacuum annealing at 600 ºC for 24 hours. First principles calculation indicates that $CoFeV_{0.5}Mn_{0.5}Si$ shows a nearly half-metallic band structure with a degree of spin polarization of about 93%. In addition, this value can be enhanced by the application of tensile strain. The room temperature x-ray diffraction patterns are indexed with the cubic crystal structure without secondary phases. The annealed sample shows ferromagnetic order with the Curie temperature well above room temperature ($T_c$ = 657 K) and a saturation magnetization of about 92 emu/g. Our results indicate that $CoFeV_{0.5}Mn_{0.5}Si$ has a potential for room temperature spin-transport-based devices.

## I. Introduction

The degree of spin polarization in electron transport is one of the key parameters taken into account for potential device applications in spin-based electronics.[1] In recent years, two types of materials have attracted particular attention for spintronic applications – half-metals and spin-gapless semiconductors (SGS). Both types of materials can potentially exhibit 100% spin polarization. The degree of spin polarization $P$ is defined as $P = \left(N_{\uparrow}(E_F) - N_{\downarrow}(E_F)\right) / \left(N_{\uparrow}(E_F) + N_{\downarrow}(E_F)\right)$, where $N_{\uparrow\downarrow}(E_F)$ is the spin-dependent density of states at the Fermi level, $E_F$.[2] Half-metals are the materials that have a semiconducting or insulating band structure for one spin, and metallic band structure for the opposite spin.[3,4,5,6,7,8,9] Spin-gapless semiconductors exhibit semiconducting or insulating band structure for one spin, and gapless band structure for the opposite spin.[10,11,12,13,14,15,16]

Materials that attracted particular attention as potential half-metals or spin-gapless semiconductors are Heusler alloys. This is mostly due to their high Curie temperature that is much larger than the room temperature.[17,18] In addition, their electronic band structure and magnetic properties can be modified by tuning the elemental compositions. Recently, quaternary Heusler alloys CoFeMnSi and CoFeVSi have been suggested to exhibit spin-gapless electronic structures.[19,20,21,22] Bainsla *et al.* performed a comprehensive experimental and computational study of CoFeMnSi and reported potential SGS properties in its completely ordered Y-type phase (prototype LiMgPdSn) based on the transport and spin-polarization measurements, as well as density functional calculations.[20] Similarly, Ren *et al.* using first principles calculations have shown that CoFeVSi in XA structure (prototype $Hg_2CuTi$) is spin-gapless semiconducting but it loses its SGS property with $L2_1B$ disorder (Co-Fe disorder), becoming a normal ferromagnetic metal.[22] CoFeMnSi exhibits both high magnetization (4.00 $\mu_B$/f.u) and high Curie temperature (826

K).[23] Although high $T_c$ is desired, high magnetization is not preferred for spintronic applications. On the other hand, CoFeVSi exhibits relatively low magnetization (2.1 $\mu_B$/f.u) but its $T_c$ (260 K) is too low for room temperature applications.[21] In the current work, we report the results of a combined experimental and theoretical investigation on $CoFeV_{0.5}Mn_{0.5}Si$, which is nearly half-metallic with an equilibrium spin polarization of about 93%. Our goal is to develop a new alloy that exhibits a moderate magnetization and sufficiently high $T_c$ for spintronic applications.

## II. Methods

### A. Experimental methods

The $CoFeV_{0.5}Mn_{0.5}Si$ bulk alloy was prepared using arc melting and vacuum annealing. Pieces cut from commercially available metal pellets matching the desired stoichiometry were melted on a water-cooled Cu hearth of an arc furnace in an argon environment. The arc melted ingot was annealed in a tubular vacuum furnace ($\sim 10^{-7}$ torr) at 600 °C for 24 hours to further homogenize the sample. The crystal structure of the sample was analyzed using Rigaku MiniFlex600 x-ray diffractometer with Cu-Kα source (λ = 1.54 Å) and magnetic properties were measured using a Quantum Design VersaLab magnetometer. The elemental composition of the annealed sample was confirmed using Energy-dispersive x-ray spectroscopy (EDS) and the measured composition is $Co_{1.00}Fe_{1.00}Mn_{0.51}V_{0.51}Si_{0.98}$, which agree well with the nominal composition.

### B. Computational methods

All calculations were performed using the Vienna *ab initio* simulation package (VASP),[24] within the projector augmented-wave method (PAW)[25] and generalized-gradient approximation

(GGA) proposed by Perdew, Burke, and Ernzerhof.[26] The cut-off energy of the plane-waves was set to 500 eV, and we used the integration method by Methfessel and Paxton with a 0.05 eV width of smearing.[27] The total energy and electronic structure calculations were performed with the energy convergence criteria of $10^{-3}$ meV. The Brillouin-zone integration was performed with a *k*-point mesh of 12 × 12 × 12. Some of the results and figures were obtained using the MedeA® software environment.[28] All calculations were performed using Extreme Science and Engineering Discovery Environment (XSEDE) resources located at the Pittsburgh Supercomputing Center (PSC),[29] and at a local computer cluster located at the University of Northern Iowa (UNI).

## III. Results and discussion

### A. Computational results

Figure 1(a) shows the atomic coordinates of $CoFeV_{0.5}Mn_{0.5}Si$. Here, in the 16-atom unit cell of CoFeMnSi (the atomic structure is reported in Ref. 20), we replace two Mn atoms with V. We note that all atomic configurations that result in 50% substitution of Mn with V are energetically equivalent in the considered geometry. The calculated density of states (DOS) of $CoFeV_{0.5}Mn_{0.5}Si$ using equilibrium lattice parameters of $a = b = 5.615$ Å; $c = 5.642$ Å are shown in Figure 1(b). Although there is a small tetragonal distortion in the unit cell, it is too small to be realized experimentally and the synthesized material should likely be cubic.

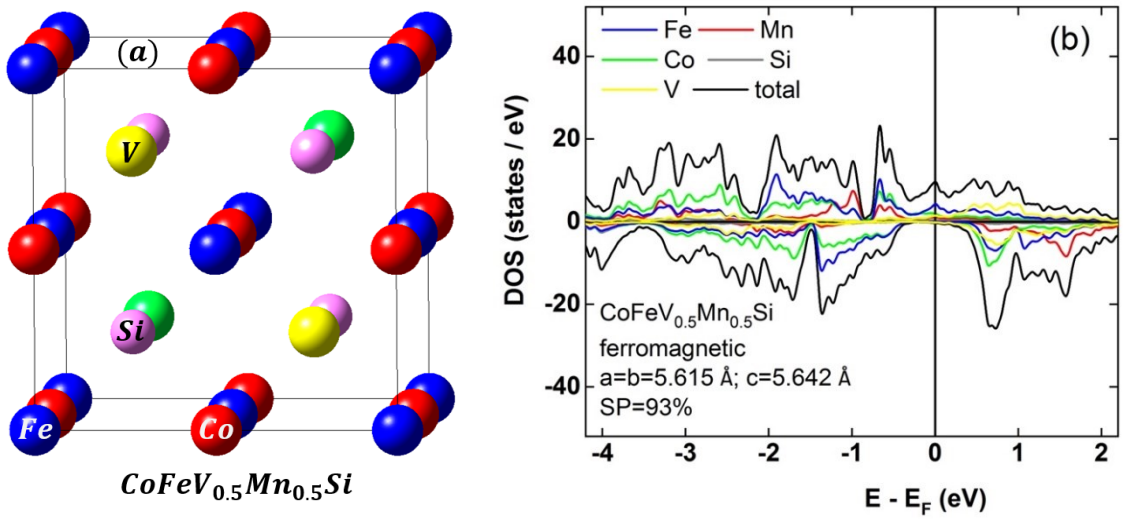


Figure 1: (a) Crystal structures of $CoFeV_{0.5}Mn_{0.5}Si$. Atoms are colored as indicated in the figure: Co – red, Fe – blue, Mn – green, V – yellow, Si – magenta (b) Calculated element- and spin-resolved density of states of bulk $CoFeV_{0.5}Mn_{0.5}Si$. The color scheme of atomic contributions is indicated in the figure and is consistent with the one used in (a). Calculated spin polarization (SP), magnetic alignment, and equilibrium lattice parameters are shown in the figure.

CoFeMnSi is predicted to exhibit a nearly SGS electronic structure, with a minority-spin band gap of around 0.65 eV, and a gapless majority-spin state.[20] As shown in Fig. 1(b), replacing half of the Mn atoms with V in CoFeMnSi destroys the gapless structure of the majority-spin states. Moreover, the energy gap of the minority-spin states of $CoFeV_{0.5}Mn_{0.5}Si$ is also reduced as a small number of vanadium states populate the Fermi level. This leads to a nearly half-metallic band-structure with a spin polarization of about 93%.

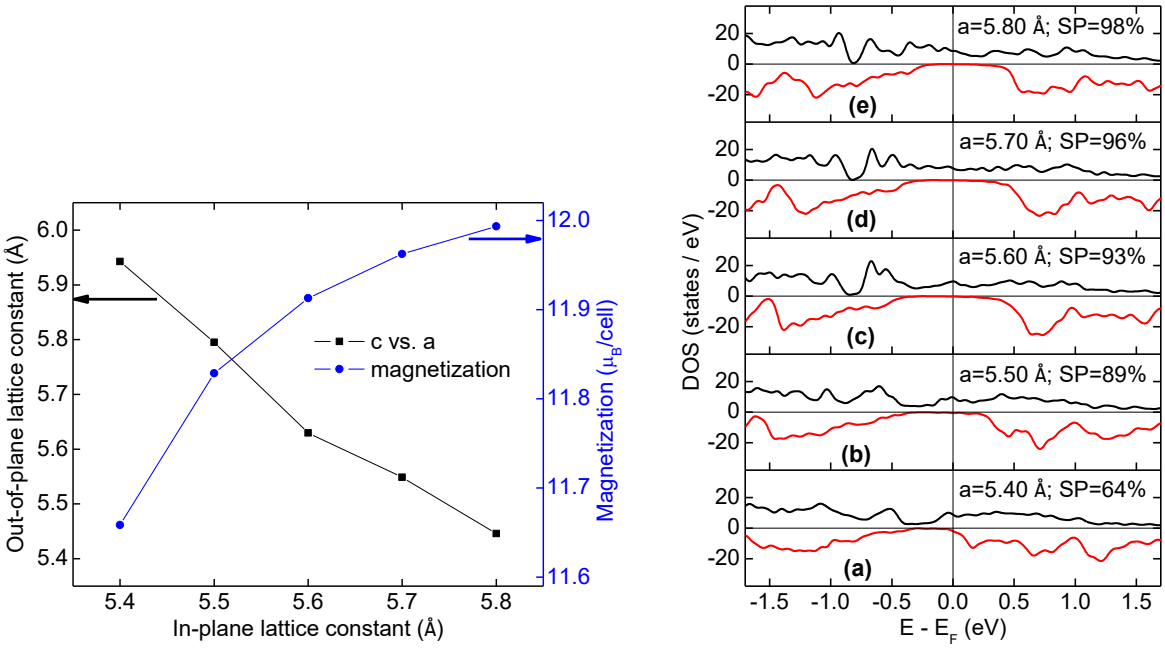


Figure 2: Left panel: calculated out-of-plane lattice constant (black line and squares), and magnetization (blue line and circles) as a function of in-plane lattice constant of $CoFeV_{0.5}Mn_{0.5}Si$ under biaxial strain. Right panel: calculated total density of states of $CoFeV_{0.5}Mn_{0.5}Si$ under biaxial strain. In-plane lattice constants and calculated spin polarization (SP) figures are shown in the figure. Positive DOS (black line) and negative DOS (red line) correspond to the majority and minority spin states, respectively.

The magnetic alignment of $CoFeV_{0.5}Mn_{0.5}Si$ is ferromagnetic, similar to the one observed in CoFeMnSi. The calculated total magnetic moment of $CoFeV_{0.5}Mn_{0.5}Si$ is 2.98 $\mu_B$/f.u, where the contributions from Co, Fe and Mn moments are about 0.94 $\mu_B$, 0.69 $\mu_B$, and 2.87 $\mu_B$, respectively. The magnetic moments of Si and V are negligible. This value of total magnetic moment is smaller than the value (4.00 $\mu_B$/f.u) reported for CoFeMnSi[20] and larger than that of CoFeVSi (2.1 $\mu_B$/f.u)[21], as expected. The integer value of the total magnetic moment is characteristic feature of a half-metal with 100% spin polarization.[30]

For spintronic applications materials in the form of films are desired. In thin-film geometry, materials are often subjected to biaxial strain, which results from a lattice mismatch with a

substrate. Electronic and magnetic properties of materials may be very sensitive to mechanical strain, which, therefore, needs to be analyzed for potential practical applications. The effect of biaxial strain on the electronic and magnetic properties of $CoFeV_{0.5}Mn_{0.5}Si$ are summarized in Fig. 2. As illustrated in the left panel of Fig. 2, application of tensile strain increases the net magnetization of $CoFeV_{0.5}Mn_{0.5}Si$, and at the largest considered lattice parameter, the magnetization is almost an integer with a value of 3.00 $\mu_B$/f.u. (12.00 $\mu_B$ per 16-atom cell). This may indicate a tendency towards half-metallicity as at 100% spin-polarization the total magnetic moment is an integer. This is confirmed by the calculated density of states and spin-polarization values, illustrated in the right panel of Fig. 2, where the in-plane lattice parameters and calculated spin-polarization values are shown. As indicated in this figure, the application of tensile strain increases the spin polarization, while the compressive strain reduces its magnitude. Specifically, at the largest considered in-plane lattice constant of 5.80 Å, the calculated spin polarization is 98%.

### B. Experimental results

Figure 3 shows the room-temperature x-ray diffraction (XRD) pattern of the annealed $CoFeV_{0.5}Mn_{0.5}Si$ alloy, which suggests that the sample is polycrystalline and crystallizes in a cubic Heusler structure. The XRD pattern contains both the fundamental and superlattice peaks expected for the ordered phase. The completely ordered quaternary Heusler alloys crystallize in the Y structure (prototype LiMgPdSn) but in practice, most of the synthesized alloys are found to crystallize in the disordered phases. In order to find the crystalline order and possible impurity phases, we analyzed the XRD pattern of the annealed sample by the Rietveld method. As shown in Fig. 3, the best fit was obtained for cubic Heuslar Y structure similar to the one predicted for ordered parent compound CoFeMnSi. The lattice parameter and density of the alloy obtained from

the Rietveld analysis are $a = 5.667$Å and $= 6.81\ g/cm^3$ , respectively. The experimental lattice parameter is close to the one predicted by our first principles calculations.

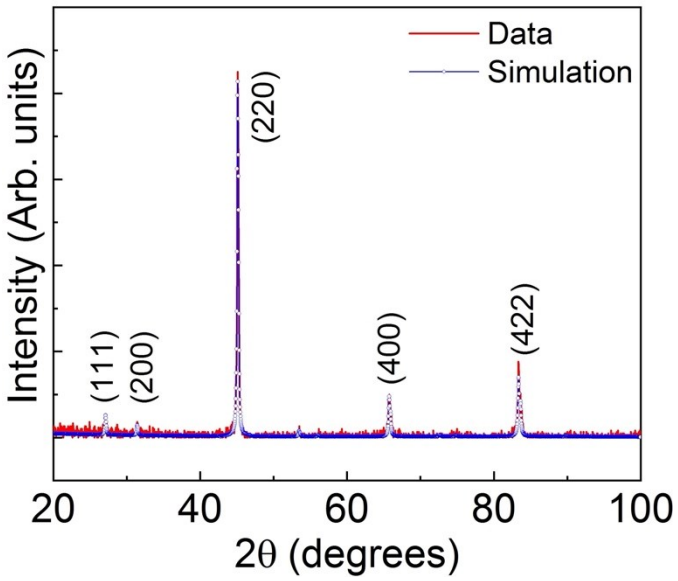


Fig. 3: Room temperature x-ray diffraction pattern recorded on $CoFeV_{0.5}Mn_{0.5}Si$. The figure includes experimental data and Rietveld simulated pattern.

Figure 4 summarizes the magnetic properties of $CoFeV_{0.5}Mn_{0.5}Si$, where the isothermal magnetization *M(H)* curve (a) and the thermomagnetic *M(T)* curve (b) are shown. The temperature dependence of magnetization measured between 50 K and 900 K indicates that $CoFeV_{0.5}Mn_{0.5}Si$ exhibits a single magnetic transition at its Curie temperature of 657 K. This value of *Tc* is much higher than room temperature and lies between the reported values for CoFeMnSi (826 K) and CoFeVSi (260 K). Qualitatively, the behavior of *Tc* in this compound is consistent with the simple mean field approximation model, where the critical temperature is directly proportional to the number of neighboring magnetic dipoles.

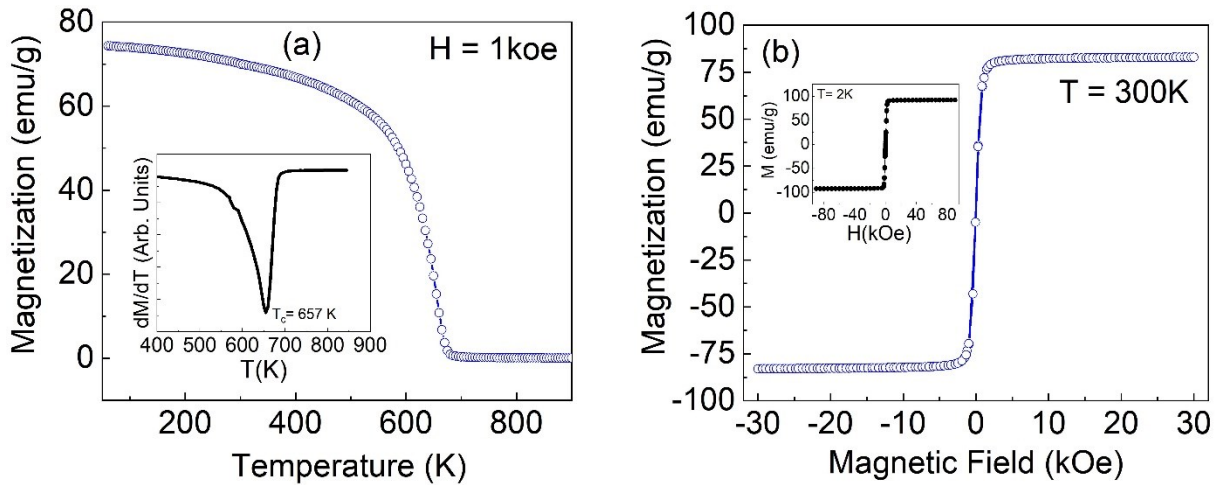


Fig. 4: The temperature (a) and field (b) dependence of magnetization of annealed $CoFeV_{0.5}Mn_{0.5}Si$ sample. The inset of figures (a) and (b) are the *M(H)* curve measured at 2K, and the *dM/dT* versus *T* showing the Curie temperature, respectively.

As shown in Fig. 4(b), the magnetic hysteresis loops measured at 300 K and 2K (inset) indicate that $CoFeV_{0.5}Mn_{0.5}Si$ is magnetically soft with the saturation magnetization of 92 emu/g (3.06 $\mu_B$/f.u). The high field (3T) magnetization measured at 300 K is 83 emu/g. The value of saturation magnetization was expressed in terms of $\mu_B$/f.u. using the lattice parameter and density of CoFeV0.5Mn0.5Si obtained from the Rietveld analysis of the XRD pattern. The experimental saturation magnetization of $CoFeV_{0.5}Mn_{0.5}Si$ is in good agreement with the value of 2.98 $\mu_B$/f.u. predicated by our first principles calculations for ferromagnetic spin order. The integral value of $M_s$ is the characteristic feature of half-metallic compounds and have been reported for other half-metallic and SGS compounds.[31]

## IV. Conclusions

In summary, we have investigated the electronic, structural, and magnetic properties of $CoFeV_{0.5}Mn_{0.5}Si$ alloy. First principles calculations indicate that $CoFeV_{0.5}Mn_{0.5}Si$ is nearly half-metallic with a degree of spin polarization of about 93%. The application of tensile strain may

further enhance this value. The arc-melted bulk sample exhibits a cubic Heusler structure without any impurity phases after annealing at 600ºC for 24 hours. At room temperature, $CoFeV_{0.5}Mn_{0.5}Si$ shows ferromagnetic order with high-field (3T) magnetization of 83 emu/g ($M_s$ = 92 emu/g at 2K) and Curie temperature of 657 K. The observed magnetic and electronic structure properties indicate that $CoFeV_{0.5}Mn_{0.5}Si$ has a potential for room temperature spin-transport-based devices.

## V. Acknowledgments

This research is supported by the *National Science Foundation* (NSF) under Grant Numbers 2003828 and 2003856 via DMR and EPSCoR. This work used the Extreme Science and Engineering Discovery Environment (XSEDE), which is supported by National Science Foundation grant number ACI-1548562. This work used the XSEDE Regular Memory (Bridges 2) and Storage (Bridges 2 Ocean) at the Pittsburgh Supercomputing Center (PSC) through allocation TG-DMR180059, and the resources of the Center for Functional Nanomaterials, which is a U.S. DOE Office of Science Facility, and the Scientific Data and Computing Center, a component of the Computational Science Initiative, at Brookhaven National Laboratory (BNL) under Contract No. DE-SC0012704.

## References

1 I. Žutić, J. Fabian, and S. Das Sarma, Rev. Mod. Phys. **76**, 323 (2004).
2 J. P. Velev, P. A. Dowben, E. Y. Tsymbal, S. J. Jenkins, and A. N. Caruso, Surf. Sci. Rep. **63**, 400 (2008).
3 R. A. de Groot, F. M. Mueller, P. G. van Engen, and K. H. J. Buschow, Phys. Rev. Lett. **50**, 2024 (1983).
4 I. Galanakis, P. H. Dederichs, N. Papanikolaou, Phys. Rev. B **66**, 174429 (2002).
5 E. Şaşıoğlu, L. M. Sandratskii, and P. Bruno, Phys. Rev. B **72**, 184415, (2005).
6 B. Balke, G. H. Fecher, J. Winterlik, and C. Felser, Appl. Phys. Lett. **90**, 152504 (2007).

[7] J. Winterlik, S. Chadov, A. Gupta, V. Alijani, T. Gasi, K. Filsinger, B. Balke, G. H. Fecher, C. A. Jenkins, F. Casper, J. Kübler, G. Liu, L. Gao, S. S. P. Parkin, and C. Felser, Adv. Mater. **24**, 6283 (2012).
[8] I. Galanakis, in *Heusler Alloys*, Springer Series in Materials Science 222, C. Felser and A. Hirohata (eds.), Springer International Publishing Switzerland 2016.
[9] P. Lukashev, P. Kharel, S. Gilbert, B. Staten, N. Hurley, R. Fuglsby, Y. Huh, S. Valloppilly, W. Zhang, K. Yang, R. Skomski, and D. J. Sellmyer, Appl. Phys. Lett. **108**, 141901 (2016).
[10] X. L. Wang, Phys. Rev. Lett. **100**, 156404 (2008).
[11] K. Ӧzdoğan, E. Şaşioğlu, and I. Galanakis, J. Appl. Phys. **113**, 193903 (2013).
[12] H. Y. Jia, X. F. Dai, L. Y. Wang, R. Liu, X. T. Wang, P. P. Li, Y. T. Cui, and G. D. Liu, AIP Adv. **4**, 047113 (2014).
[13] P. Kharel, W. Zhang, R. Skomski, S. Valloppilly, Y. Huh, R. Fuglsby, S. Gilbert, and D. J. Sellmyer, Phys. D: Appl. Phys. **48**, 245002 (2015).
[14] S. Ouardi, G. H. Fecher, and C. Felser, Phys. Rev. Lett. **110**, 100401 (2013).
[15] A. Nelson, P. Kharel, Y. Huh, R. Fuglsby, J. Guenther, W. Zhang, B. Staten, P. Lukashev, S. Valloppilly, and D. J. Sellmyer, J. Appl. Phys. **117**, 153906 (2015).
[16] S. Skaftouros, K. Ӧzdoğan, E. Şaşioğlu, and I. Galanakis, Appl. Phys. Lett. **102**, 022402 (2013).
[17] T. Ishikawa, N. Itabashi, T. Taira, K. Matsuda, T. Uemura, and M. Yamamoto, J. Appl. Phys. **105**, 07B110 (2009).
[18] M. Jourdan et al., Nature Communications **5**, 3974 (2014).
[19] G. Xu, E. Liu, Y. Du, G. Li, G. Liu, W. Wang, and G. Wu, EPL **102**, 17007 (2013).
[20] L. Bainsla, A. Mallick, M. Manivel Raja, A. Nigam, B. Varaprasad, Y. Takahashi, A. Alam, K. Suresh, and K. Hono, Phys. Rev. B **91**, 104408 (2015).
[21] S. Yamada, S. Kobayashi, F. Kuroda, K. Kudo, S. Abo, T. Fukushima, T. Oguchi, and K. Hamaya, Phys. Rev. Materials **2**, 124403 (2018).
[22] Z. Ren, Y. Zhao, J. Jiao, N. Zheng, H. Liu and S. Li, J Supercond Nov Magn, **29**, 3181 (2016).
[23] C. You, H. Fu, Y. Li, Z. Ou, L. Ma, N. Tian, V. Wang, Materials Research Bulletin **133**, 111044 (2021).
[24] G. Kresse and D. Joubert, Phys. Rev. B **59**, 1758 (1999).
[25] P. Blöchl, Phys. Rev. B **50**, 17953 (1994).
[26] J. P. Perdew, K. Burke, and M. Ernzerhof, Phys. Rev. Lett. **77**, 3865 (1996).
[27] M. Methfessel and A. T. Paxton, Phys. Rev. B **40**, 3616 (1989).
[28] MedeA-2.22, Materials Design, Inc., San Diego, CA, USA, 2017.
[29] J. Towns, T. Cockerill, M. Dahan, I. Foster, K. Gaither, A. Grimshaw, V. Hazlewood, S. Lathrop, D. Lifka, G. D. Peterson, R. Roskies, J. R. Scott, N. Wilkins-Diehr, "XSEDE: Accelerating Scientific Discovery", Computing in Science & Engineering, vol.**16**, no. 5, pp. 62-74, Sept.-Oct. 2014.
[30] I. Tutic, J. Herran, B. Staten, P. Gray, T. Paudel, A. Sokolov, E. Tsymbal, and P. Lukashev, J. Phys.: Condens. Matter **29**, 075801 (2017).
[31] E. O'Leary, A. Ramker, D. VanBrogen, B. Dahal, E. Montgomery, S. Poddar, P. Kharel, A. Stollenwerk, and P. Lukashev, J. Appl. Phys., **128**, 113906 (2020)